Polymer Testing 31 (2012) 723–727

Contents lists available at SciVerse ScienceDirect

Polymer Testing

journal homepage: www.elsevier.com/locate/polytest

Test method

# The effect of strain rate on the mechanical behavior of Teflon foam

A. Tasdemirci*, A.K. Turan, M. Guden

*Dynamic Testing and Modeling Laboratory, Department of Mechanical Engineering, Izmir Institute of Technology, Gulbahce, Urla, Izmir 35430, Turkey*

ARTICLE INFO

*Article history:*
Received 30 March 2012
Accepted 12 May 2012

*Keywords:*
Split Hopkinson Pressure Bar
Quartz crystal
Strain rate sensitivity
LS-DYNA

ABSTRACT

The quasi-static ($1 \times 10^{-3}$, $1 \times 10^{-2}$ and $1 \times 10^{-1}$ $s^{-1}$) and high strain rate (7200 and 9500 $s^{-1}$) experimental and high strain rate numerical compression deformation of a Gore Polarchip™ CP7003 heat insulating Teflon foam was investigated. High strain rate tests were conducted with the insertion of quartz crystal piezoelectric transducers at the end of the transmitter bar of a compression Split Hopkinson Pressure Bar (SHPB) set-up in order to measure the force at the back face of the specimen. A fully developed numerical model of the SHPB test on Teflon was also implemented using LS-DYNA. The simulation stresses showed close correlations with the experimentally measured stresses on the bars. The developed model successfully simulated the high strain rate loading. The damage initiation and progression of experimental high strain rate tests were further recorded using a high speed camera and found to be very similar to those of the simulation high strain rate tests.


## 1. Introduction

Soft materials are distinguished by low mechanical impedance and low strength. In addition to many other applications, these materials are used where impact or shock loadings can occur. A well-known example for these applications is the rubber inter-layer between composite backing plate and ceramic front face of integrated composite armor [1,2]. The rubber inter-layer in the composite armor functions to distribute the incoming projectile momentum to a wider area of the continuous backing composite plate, diminishing the damage. In these applications, a thorough knowledge of the mechanical behavior of soft materials at increasingly high strain rates is certainly a prerequisite. In parallel with this, a dependable laboratory scale experimental set-up is also needed to mimic the actual impact loading conditions. The Split Hopkinson Pressure Bar (SHPB), originally developed by Kolsky in 1949 [3], is a widely used experimental method of testing a wide range of material groups, including composites [4], metals [5], ceramics [6] and viscous fluids [7], at strain rates higher than ~100 $s^{-1}$. Nevertheless, testing soft materials using SHPB is known to be problematic because of the impedance mismatch between the test and bar materials. In testing soft materials such as polymers, the transmitter bar signal is usually weak, leading to difficulties in distinguishing the experimental signals from noise.

Various solutions to overcome this problem have been reported. An SHPB set-up made of viscoelastic bars was implemented in order to cover the impedance mismatch disadvantage of soft specimens; however, the nature of viscoelasticity of the bar materials resulted in intensified wave dispersion and attenuation effects [8,9]. The use of hollow SHPB transmitter bars was also investigated but it did not affect the amplitude of the noise [10]. The classical SHPB set-up was modified to test soft materials by measuring the sample forces by means of piezoelectric transducers [11–15]. With the insertion of quartz crystals at the impact ends of the incident and transmitter bars, the forces at the front and back of the specimen were measured directly and dynamic equilibrium was maintained throughout the experiment; hence, the validity of the tests was checked.

* Corresponding author. Tel.: +90 232 7506780; fax: +90 232 7506701.
*E-mail address:* alpertasdemirci@iyte.edu.tr (A. Tasdemirci).

0142-9418/$ – see front matter © 2012 Elsevier Ltd. All rights reserved.
doi:10.1016/j.polymertesting.2012.05.004

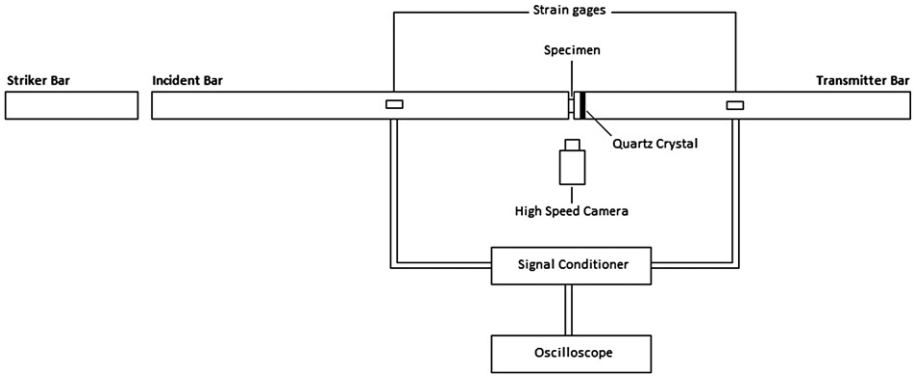


**Fig. 1.** Schematic of modified SHPB set-up.

In this study, an optimized method for the dynamic measurement of stress through the SHPB testing of Gore Polarchip CP7003 polymeric foam by inserting quartz crystals at the impact end of the transmitter bar was investigated experimentally and numerically. The results of classical SHPB stress calculations were then compared with those measured using quartz crystals. In parallel with these experimental efforts, a fully developed numerical model of SHPB test was implemented using LS–DYNA.

## 2. Experimental

Gore Polarchip™ 7003 Teflon thermal insulator foam sheets were received in 2 mm thickness from which compression test samples, 12 mm in diameter and 2 mm in thickness, were core-drilled. Quasi–static compression tests were conducted in a Shimadzu AG test machine at strain rates of $10^{-3}$, $10^{-2}$ and $10^{-1}$ $s^{-1}$. High strain rate compression tests were performed in a modified 7075-T6 aluminum SHPB set-up as shown schematically in Fig. 1. In a classical SHPB set-up, a cylindrical sample is sandwiched between incident and transmitter bars by a compressive elastic stress wave which is created by the impact of a striker bar on the end of the incident bar. The magnitude and amplitude of the stress waves on the incident and transmitter bars are measured by means of the strain gages mounted on the bars. The strain ($\varepsilon$), stress ($\sigma$) and strain rate ($\dot{\varepsilon}$) of the sample are calculated using the following relations

$$\varepsilon(t) = -\frac{2C_b}{L_s}\int_0^t \varepsilon_r(t)dt \tag{1}$$

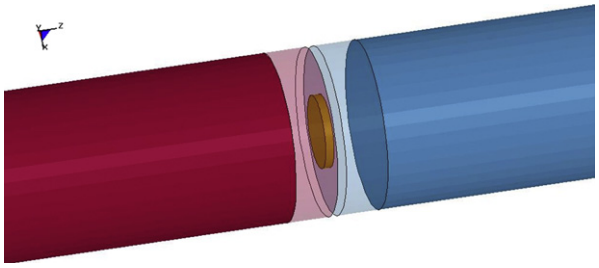

**Fig. 2.** Finite element model of Teflon specimen between incident and transmitter bars.

$$\sigma(t) = \frac{E_b A_b}{A_s}\varepsilon_t(t) \tag{2}$$

$$\dot{\varepsilon}(t) = -\frac{2C_b}{L_s}\varepsilon_r(t) \tag{3}$$

where $C_b$ is the wave velocity of the bar, $E_b$ is the elastic modulus of the bar, $L_s$ is the specimen length and $A_b$ and $A_s$ are the bar and specimen cross-sectional areas, respectively. The measured strains on the incident and transmitter bars, $\varepsilon_r$ and $\varepsilon_t$, refer to the reflected and transmitted strains, respectively. The SHPB 7075-T6 aluminum striker, incident and transmitter bars had a diameter of 40 mm and the lengths of 300 mm, 2000 mm and 1000 mm, respectively. A quartz crystal piezoelectric transducer was inserted at the impact end of the transmitter bar in order to measure the force on the sample directly during an experiment (Fig. 1). The selected X–cut quartz crystal was 40.00 ± 0.01 mm in diameter and 0.254 ± 0.01 mm in thickness and had a mechanical impedance very similar to that of the bar material (bar: $14.19 \times 10^6$ kg $m^{-1}$ $s^{-2}$, quartz: $15.11 \times 10^6$ kg $m^{-1}s^{-2}$ and the ratio: 1.06). The quartz crystal was bonded to the impact end of transmitter bar using a conductive epoxy (Circuit Works CW 2400) and covered with a thin aluminum disc in order to prevent damaging during the experiment. The piezoelectric constant of the quartz crystal was $-2.3 \times 10^{-12}$ C $N^{-1}$, as specified by the manufacturer [16]. The signals gathered from quartz crystals during an experiment were measured by means of a Kistler 5010A charge amplifier. The signals were recorded in a LDS Genesis data acquisition system, while real time deformation of the test sample under high strain rate loading was captured using a Photron FastCam high speed camera.

## 3. Modeling

SHPB compression tests were simulated using the LS–DYNA 971 finite element program. The fully developed

**Table 1**
Properties of bar material used in finite element analysis.

| Material | Modulus of Elasticity (GPa) | Poisson's ratio | Density (kg $m^{-3}$) | Other |
|---|---|---|---|---|
| Aluminum 7075–T6 | 71.7 | 0.33 | 2810 | – |

**Table 2**
Material properties used in numerical model for Teflon.

| Material | Modulus of Elasticity (GPa) | Poisson's ratio | Density (kg m$^{-3}$) | Other |
|---|---|---|---|---|
| Teflon | 3.65 | 0.01 | 760 | TSC = 50 MPa DAMP = 0.05 |

numerical model (Fig. 2) consisted of 316,200 total elements, 120,000 elements for incident and transmitter bars. The mesh size was optimized by cross-checking the transmitter bar data of three different mesh densities, 0.255, 0.225 and 0.2 mm, to reduce CPU time. The optimum mesh size was determined to be 0.2 mm. The test sample, Teflon, was modeled using MAT_063 failure model. This isotropic crushing failure model is dedicated to simulate crushable foams with optional parameters such as tension cut–off stress and damping coefficient. Through the numerical study, the tension cut–off stress was taken as 50 MPa and the damping coefficient as 0.05. Material properties of the finite element analysis of the bar and Teflon are tabulated in Tables 1 and 2, respectively. The experimental stress-strain curves of Teflon at a specific strain rate were used as an input to LSDYNA.

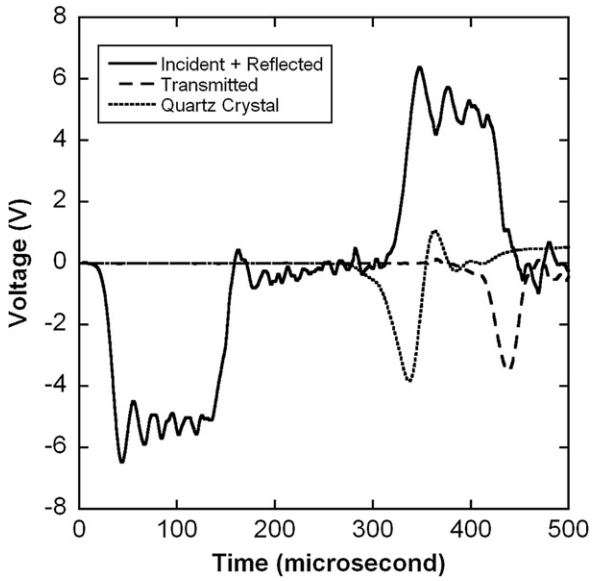


**Fig. 3.** Experimental data recorded from modified SHPB at 7200 s$^{-1}$.

## 4. Results and discussion

Typical SHPB experimental data recorded at high strain rates is shown in Fig. 3. Solid and dashed lines in Fig. 3 represent the signals recorded with strain gages mounted on the incident and transmitter bar, respectively, while the dotted line represents the signal recorded with the quartz crystal. The signals measured using strain gage and quartz crystal, as seen in Fig. 3, are very much similar in shape and amplitude. High strain–rate compression stress-strain curves of Teflon at 7200 s$^{-1}$ and 9500 s$^{-1}$ are shown in Fig. 4(a) and (b) respectively. As seen in the same figures, the strain gage measurements of stress results in oscillations at relatively low strains, overshooting stress up to strain level of 0.08 and underestimating the stress of specimen up to the strain of 0.15. High strain rate stress–strain curves also show that measured strain gage and quartz crystal stress values approach each other after 0.15 strain. The compression stress-strain curves at quasi-static and high strain rates regimes are shown together in Fig. 5. As the strain rate increases, the Teflon material stiffens faster, showing a strong strain–rate dependency. Densification strain of Teflon also decreases with increasing strain rate; the specimen stress is about 15 MPa at about 0.8 at $10^{-3}$ s$^{-1}$, while the strain is reduced to 0.1 at a stress level at 9500 s$^{-1}$.

The SHPB responses of the developed model and experiments conducted at the same strain rate are shown in Fig. 6. In the same figure, the numerical response is shifted on the time axis for easy comparison. As seen in Fig. 6, the numerical bar responses of incident and transmitter bars are very similar to experimental bar responses, showing good correlation between model and experiments

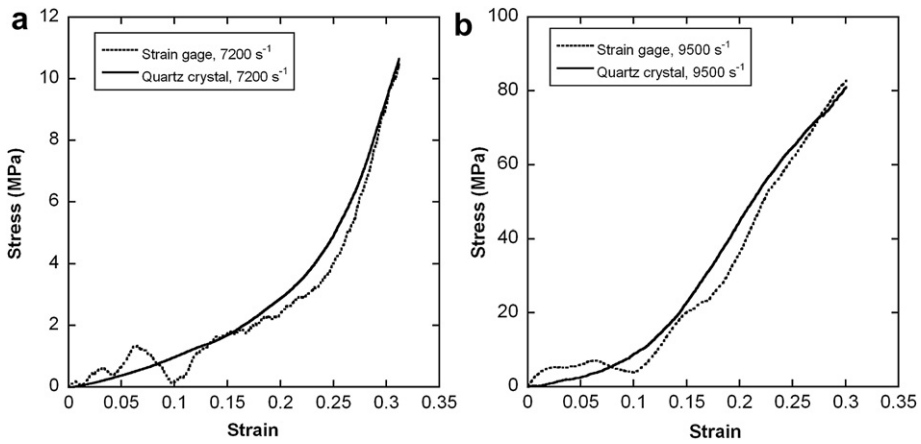


**Fig. 4.** Comparison of stress-strain curves determined from strain gage and quartz crystal at (a) 7200 s$^{-1}$ and (b) 9500 s$^{-1}$.

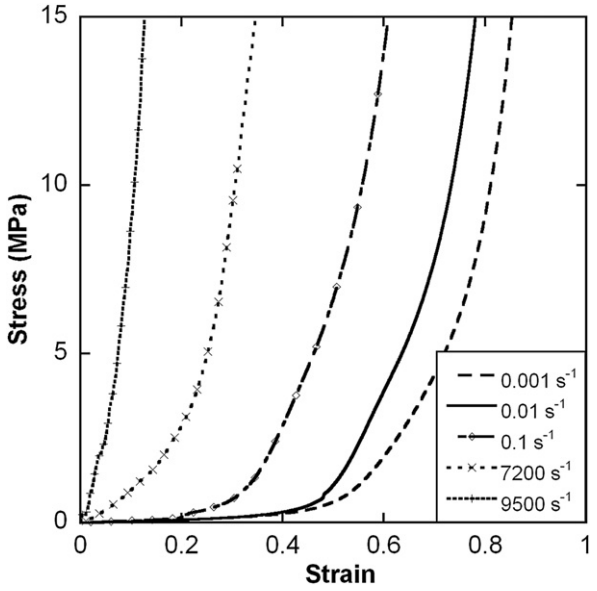


**Fig. 5.** Stress strain curves at quasi-static and high strain rates.

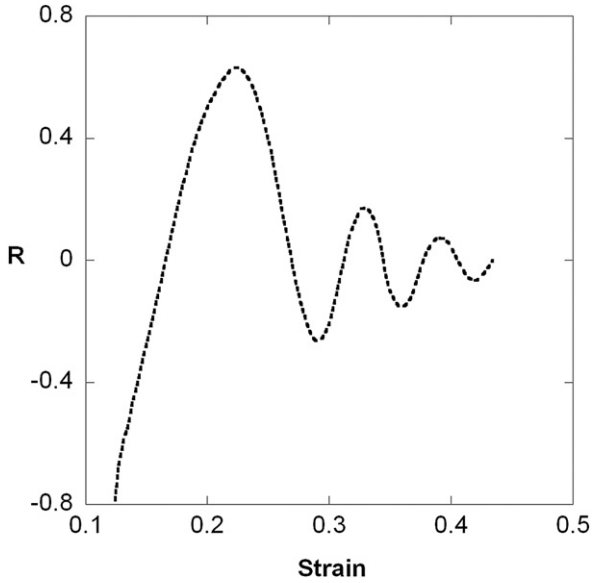


**Fig. 7.** Numerical dimensionless $R$ parameter-strain graph at 7200 $s^{-1}$.

both in magnitude and amplitude of incident and transmitted bar stress waves.

Experiments in SHPB are only valid if there is force equilibrium at the front and back face of the specimen, and this state is checked with a dimensionless parameter $R$ defined as

$$R = -\frac{2(F_1 - F_2)}{(F_1 + F_2)} \tag{4}$$

where, $F_1$ and $F_2$ are the forces measured at the front and back face of the specimen, respectively. $R$ parameter represents the extent of deviation of stress equilibrium in the specimen. When the value of $R$ reaches 0, stress equilibrium is reached in the material. The variation of numerical $R$ parameter with strain in a Teflon sample tested at 7200 $s^{-1}$ is shown in Fig. 7. As seen in the same figure, the value of $R$ converges to 0 at a strain level of 0.35, after which the stress equilibrium is reached in the specimen. The experimental and numerical SHPB transmitter bar force-time curves are shown in Fig. 8 for comparison. Both curves tend to follow the similar trends up to 280 μs, while the numerical force values are slightly greater than experimental force values. A greater correlation between experimental and numeric force values are seen up to 310 μs.

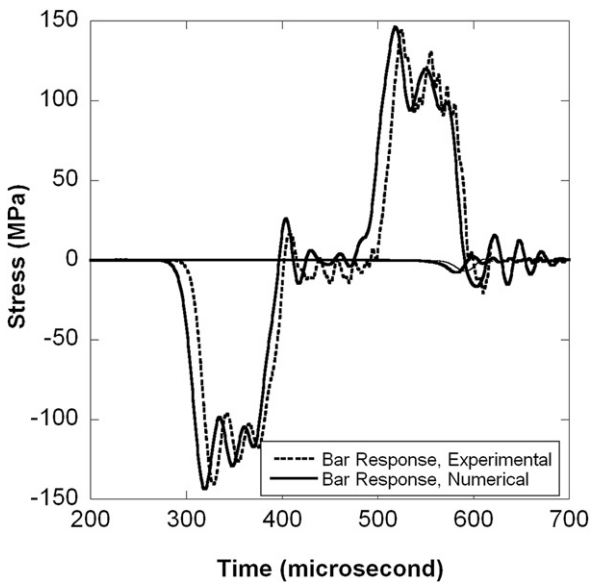


**Fig. 6.** Comparison of bar responses of experiment and model at 7200 $s^{-1}$.

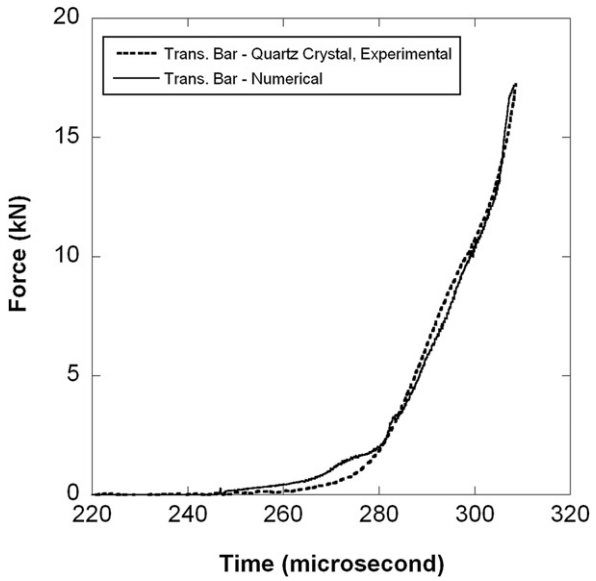


**Fig. 8.** Comparison of numerical and experimental forces on the transmitter bar at 7200 $s^{-1}$.

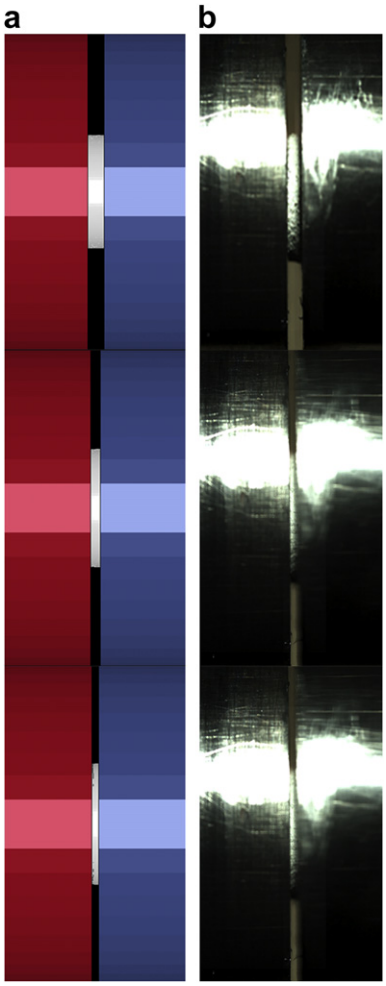


**Fig. 9.** Comparison of damage behavior a) numerical model and b) experiment at 9500 $s^{-1}$.

The numerical and real time SHPB Teflon sample pictures at various deformation times are shown in Fig. 9(a) and (b). Non-deformed numerical samples are seen at 0 μs. At 92 μs, as the stress wave travels through the incident bar, the specimen is compressed between incident and transmitted bars and expanding vertically while the length of the specimen is reduced. At 184 μs, the sample is fully deformed and tends to lose shape completely while being smeared between incident and transmitted bars. Significant change in the transmitter bar's position is not observed through the experiments since the Teflon is a soft material which absorbs the stress wave.

## 5. Conclusions

The experimental and numerical quasi-static and high strain rate compression deformation of a Gore Polarchip™ CP7003 heat insulating Teflon foam was investigated. High strain rate tests were conducted with a modified SHPB, in which quartz crystals were bonded to the impact end of transmitter bar to measure the force at the back face of specimen directly. A strong strain rate dependency in the flow stress of Teflon was found; the stresses increased with increasing strain rate. A fully developed numerical model of SHPB testing showed good correlations with the experiments and successfully duplicated high strain rate loading conditions. Real time recordings of high strain rate deformation also showed close agreement with numerical high strain rate deformation in damage initiation and progression.

## Acknowledgements

The authors would like to thank the Scientific and Technical Council of Turkey (TUBITAK) for the grant # 106M353. The authors thank W.L. Gore & Associates Inc. for provision of the Teflon (Polarchip™) and Dr. Ian W. Hall for supplying Teflon (Polarchip™) layers.

## References

[1] H. Mahfuz, Y. Zhu, A. Haque, A. Abutalib, U. Vaidya, S. Jeelani, B. Gama, J. Gillespie, B. Fink, Investigation of high-velocity impact on integral armor using finite element method, International Journal of Impact Engineering 24 (2000) 203–217.
[2] A. Tasdemirci, G. Tunusoglu, M. Güden, The effect of the interlayer on the ballistic performance of ceramic/composite armors: experimental and numerical study, International Journal of Impact Engineering 44 (2012) 1–9.
[3] H. Kolsky, An investigation of the mechanical properties of materials at very high rates of loading, Proceedings of the Physical Society, Section B 62 (1949) 676.
[4] H. Hsiao, I. Daniel, R. Cordes, Dynamic compressive behavior of thick composite materials, Experimental Mechanics 38 (1998) 172–180.
[5] R.J. Clifton, High strain rate behavior of metals, Applied Mechanics Reviews 43 (1990) S9–S22.
[6] J. Lankford, W.W. Predebon, J.M. Staehler, G. Subhash, B.J. Pletka, C. E. Anderson, The role of plasticity as a limiting factor in the compressive failure of high strength ceramics, Mechanics of Materials 29 (1998) 205–218.
[7] A.S. Lim, S.L. Lopatnikov, J.W. Gillespie Jr., Development of the split-Hopkinson pressure bar technique for viscous fluid characterization, Polymer Testing 28 (2009) 891–900.
[8] L. Wang, K. Labibes, Z. Azari, G. Pluvinage, Generalization of split Hopkinson bar technique to use viscoelastic bars, International Journal of Impact Engineering 15 (1994) 669–686.
[9] H. Zhao, G. Gary, J.R. Klepaczko, On the use of a viscoelastic split Hopkinson pressure bar, International Journal of Impact Engineering 19 (1997) 319–330.
[10] W. Chen, B. Zhang, M. Forrestal, A split Hopkinson bar technique for low-impedance materials, Experimental Mechanics 39 (1999) 81–85.
[11] W. Chen, F. Lu, B. Zhou, A quartz-crystal-embedded split Hopkinson pressure bar for soft materials, Experimental Mechanics 40 (2000) 1–6.
[12] W. Chen, F. Lu, N. Winfree, High-strain-rate compressive behavior of a rigid polyurethane foam with various densities, Experimental Mechanics 42 (2002) 65–73.
[13] B. Song, Strain-rate effects on elastic and early cell-collapse responses of a polystyrene foam, International Journal of Impact Engineering 31 (2005) 509–521.
[14] B. Song, W. Chen, Y. Ge, T. Weerasooriya, Dynamic and quasi-static compressive response of porcine muscle, Journal of Biomechanics 40 (2007) 2999–3005.
[15] F. Pervin, W.W. Chen, T. Weerasooriya, Dynamic compressive response of bovine liver tissues, Journal of the Mechanical Behavior of Biomedical Materials 4 (2011) 76–84.
[16] Boston Piezo-Optics Inc., Mechanical Properties of Quartz Crystal, MA, USA, http://bostonpiezooptics.com/?D=27.